PCCP

Accepted Manuscript

ROYAL SOCIETY OF CHEMISTRY

www.rsc.org/pccp

Simulation of metal-organic framework self-assembly †

Makoto Yoneya *, Seiji Tsuzuki and Masaru Aoyagi

Received Xth XXXXXXXXXX 20XX, Accepted Xth XXXXXXXXX 20XX
First published on the web Xth XXXXXXXXXX 200X
DOI: 10.1039/b000000x

Spontaneous growth of metal-organic frameworks (MOFs) composed of metal ions and 4,4'-bipyridine ligands was successfully demonstrated by molecular dynamics simulations, starting from a random initial placement of the metals and the ligands. The effect of the metal-ligand binding strength upon the MOF self-assembly was investigated. We found that the metal-ligand binding strength should be within a window around the optimum values for the regular MOF growth.

Coordination directed self-assembly of metal-organic materials has attracted much interest for their science and applications[1]. In these coordination systems, both finite supramolecular complexes and infinite polymer networks are possible via self-assembly with the appropriate metal-ligand system design[2,3]. Well-known examples are the finite spherical complex $Pd(II)_{12}L_{24}$ composed of 12 palladium ions (Pd(II)) and 24 bent ligands (L in Fig. 1(a))[2] and the two-dimensional (2-D) like infinite network composed of cadmium ions and linear ligands, 4,4'-bipyridine (bpy, Fig. 1(b))[4]. The latter type 2-D like or 3-D infinite coordination polymer networks, which are also known as metal-organic frameworks (MOFs), have been extensively studied over the last decade for their various applications[5,6]. However, only a limited number of experimental studies[7,8] have been reported to date on their growth process.

In this study, we applied molecular simulation to investigate the growth process of MOFs for the first time to the best of our knowledge. A molecular simulation model[9] developed for the self-assembly of the finite complex $Pd(II)_{12}L_{24}$ was applied to infinite MOFs. In this model, the cationic dummy atom method[10] was employed to simulate coordination bond formations and dissociations. A coarse-grained solvent model was used to fill the gap between the time-scale of the coordination-directed self-assembly and that accessible by common molecular dynamics simulation[11].

We first tried to simulate 2-D like MOF self-assembly using our previous simulation model for $Pd(II)_{12}L_{24}$ by simply changing the ligand from the bent form in $Pd(II)_{12}L_{24}$ (Fig. 1(a)) to the linear form 4,4'-bpy (Fig. 1(b)) in dimethyl sulfoxide (DMSO). The DMSO solvent was treated implicitly as a continuum medium with a far-field relative dielectric constant of 47.0. The simulation temperature was maintained at room temperature (293 K) by coupling to a stochastic thermostat[9,11]. The initial structure was made by random placement of 384 Pd(II) ions and 768 4,4'-bipyridine (bpy) ligands in the cubic simulation cell with a volume of (60^3 nm^3), as shown in Fig. 2(a). We note again that the coarse-grained solvent was used to accelerate the coordination-directed self-assembly. In principle, the time scale in coarse-grained model is not "real" one, but "coarse-grained" time scale because of their acceleration dynamics[12] and so in our model. Detailed descriptions of the simulation methods are found in the supporting information of this paper.

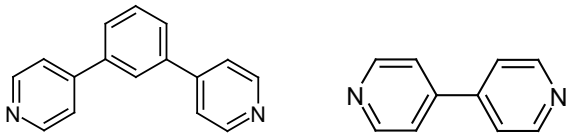

(a) (b)

Fig. 1 (a) 4,4'-benzene-1,3-diyldipyridine (L) and (b) 4,4'-bipyridine (bpy).

The simulated time evolution of the total number of coordination bonds (judged from the distance between the Pd atoms and the nitrogen atoms of the ligands Pd-N_{bpy} using the appropriate threshold[11]) is shown in Fig. 3 with a solid black line. It shows saturating behavior after ca. 0.2 μs, which implies that the coordination bonding rates are strongly dependent on the number density of the unbound pyridine rings (see Fig. S1 of the supporting information). Then, to increase the bonding rates, we shrunk the simulation box volume (ca. -1.0 %/ns) after 0.4 μs, as shown in the box volume change in Fig. 3 with a black dashed line[13,14]. With this box shrinkage, the number of four-coordinated Pd(II) was increased and the total number of the coordination bonds approached its full-bonding values, as shown in Fig. 3.

Here, we note the effect of the metal-ligand binding

0 † Electronic Supplementary Information (ESI) available: [Simulation methods, Metal-ligand binding energy, Bonding rates and density of the unbound pyridine rings, Topology file.]. See DOI: 10.1039/b000000x/

0 *a Nanosystem Research Institute, National Institute of Advanced Industrial Science and Technology, 1-1-1 Umezono, Tsukuba 305-8568, JAPAN E-mail: makoto-yoneya@aist.go.jp*

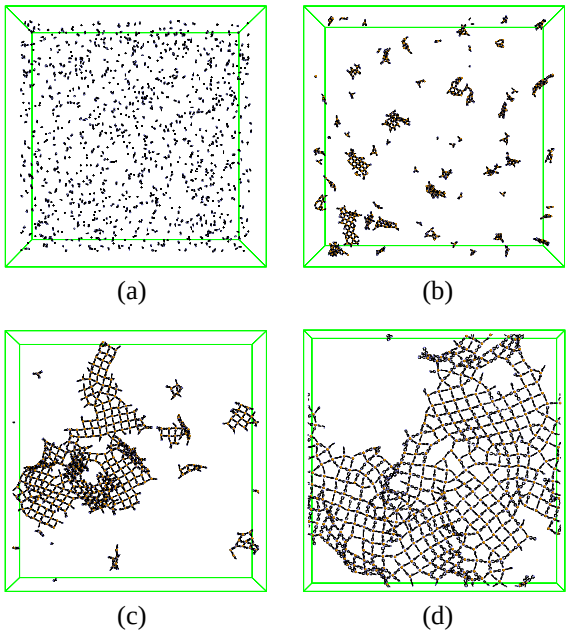

Fig. 2 (a) Initial structure and snapshot after (b) 0.4 μs, (c) 0.6 μs and (d) 0.8 μs of [Pd(II)(4,4'-bpy)$_2$] system simulation viewing along the z-axis (hydrogen atoms are omitted for clarity). The green box corresponds to the simulation box with 3-D periodic boundary conditions. The box sizes and shapes are different after 0.4 μs.

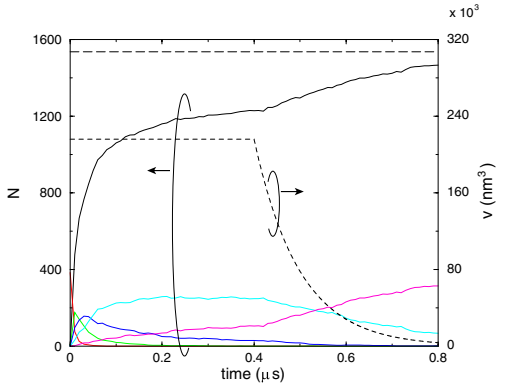

Fig. 3 Time evolution of the number of coordination bonds (black line) and number of zero- to four-coordinated (red, green, blue, cyan and magenta lines, respectively) Pd(II) and the simulation box volume (black dashed line) in the self-assembly process of the [Pd(II)(4,4'-bpy)$_2$] system. The dashed horizontal line at N=1536=2×768 corresponds to the full-bonding limit of the total coordination bonds.

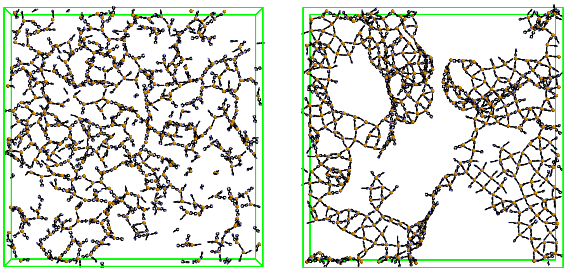

Fig. 4 Snapshot after 0.8 μs of [Pd(II)(4,4'-bpy)$_2$] system simulation with (a) ε_r = 4.0 and (b) ε_r = 1.0 (hydrogen atoms are omitted for clarity).

strength upon the MOF self-assembly. In our model, the metal-ligand binding was modeled with Coulomb potentials, $q_i q_j/(4\pi\varepsilon_r r_{ij})$, and the near-field relative dielectric constant ε_r can be regarded as a scaling parameter of the binding energy. As described previously, the far-field relative dielectric constant (ε_{rf}) was specified as 47.0 for the DMSO solvent. A polar solvent such as DMSO could behave like a ligand and enhances the metal-ligand exchange probability (effectively decrease the metal-ligand binding energy). Common choice of ε_r = 1 which corresponds to the vacuum is inadequate in this situation, because this completely neglects pseudo-ligand effect of the DMSO solvent. This pseudo-ligand effect of the polar solvent could be parameterized as the enlarged ε_r than one that (ε_r = 1) corresponds to the vacuum[11]. Fig. 4 shows the corresponding snapshots after 0.8 μs with the larger (ε_r = 4.0) and the smaller (ε_r = 1.0) near-field relative dielectric constant than the previous setting of ε_r = 2.5 in Fig. 2(d). In comparison to the Fig. 2(d) (ε_r = 2.5), Fig. 4(a) (ε_r = 4.0) shows only small clusters with mostly up to three-coordinated Pd(II) complexes because of the smaller metal-ligand binding energy. In contrast, Fig. 4(b) with the smaller ε_r = 1.0, which means the larger metal-ligand binding energy, shows more irregular deformed (e.g., triangular) networks compare to the much regular square networks in Fig. 2(d). In the current model, regular networks were obtained with $\varepsilon_r \sim$ 2–3. This corresponds to the metal-ligand binding strength should be within a window of $\pm$ 20 % around the optimum values for the regular MOF growth.

Next, we considered the 3-D extension of the 2-D like MOF described above using octahedral metal centers. With the use of [9]ane-S$_3$ capped hexacoordinated ruthenium ions and 4,4'-bpys, the formation of a supramolecular cube {([9]ane-S$_3$)Ru(II)}$_8$(4,4'-bpy)$_{12}$ in nitromethane was reported[15]. Removal of the capping groups may give an infinite 3-D cubic network, because an analogous octahedrally coordinated pyridine (py) complex Ru(II)(py)$_6$ has been previously reported[16]. However, no such 3-D MOFs consisting of only the octahedral centers and the 4,4'-bpys have been reported to date[3]. We then tried the corresponding simulation for the system.

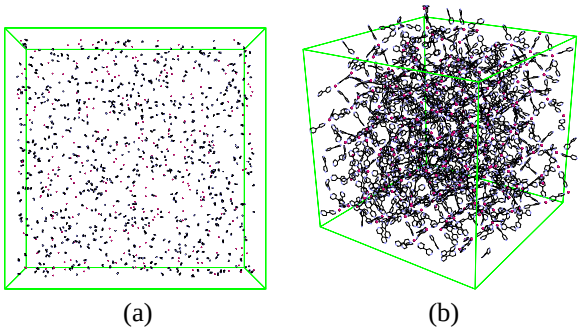

Fig. 5 (a) Initial structure and snapshot after (b) 1.0 μs of the [Ru(II)(4,4'-bpy)$_3$] system simulation (hydrogen atoms are omitted for clarity). Scale (box sizes) are different in these snapshots.

The Ru(II) ion's nonbonding parameters were taken from the universal force field (UFF)[17], and the van der Waals bond length (originally 0.2963 nm) was scaled by 0.78 to reproduce the Ru-N$_{py,bpy}$ distance (ca. 0.21 nm) from the XRD studies[15,16]. The solvent, nitromethane, was treated implicitly as a continuum medium with the far- and near-field relative dielectric constant of 36.2 and 1.75, respectively. The initial structure (Fig. 5(a)) was made by random placement of 256 Ru(II) ions and 768 4,4'-bpy ligands in the cubic simulation box with the same volume (60^3 nm^3) as in the previous system.

The time evolution of the total number of coordination bonds and the number of zero- to six-coordinated Ru(II) is shown in Fig. 6(a). Though we applied the same box shrinkage rate after 0.4 μs as used in the previous case[18], up to five-coordinated Ru(II) complexes were obtained without any six-coordinated ones. Additionally, the total coordination bond number was saturated at much lower values, and the snapshot after 1.0 μs (Fig. 5(b)) shows disordered non-regular networks. This result may be consistent with the lack of experimental reports of 3-D MOFs consisting of Ru(II) ions and 4,4'-bpys noted above.

Then, we tried to identify the key design factor to realize regular 3-D MOFs using the current simulation model as a tool. The clue for this was the previously reported 3-D cubic MOF composed of silver (Ag) ions and pyrazine (pyz) ligands[19]. In this system, relatively long Ag-N$_{pyz}$ distances of ca. 0.25 nm were obtained by XRD measurements[19]. This length is larger than the reported Ru-N$_{bpy}$ distance of ca. 0.21 nm[15], which we had fit the Ru(II) van der Waals bond length parameter in the simulation above to. Because the octahedrally coordinated structure with six 4,4'-bpys is sterically more crowded than the planar four-coordination center, a larger *M*-N$_{bpy}$ distance would be required[20–22].

To validate this, we resized the Ru(II) van der Waals bond length parameter to the Ru-N$_{bpy}$ distance of ca. 0.255 nm

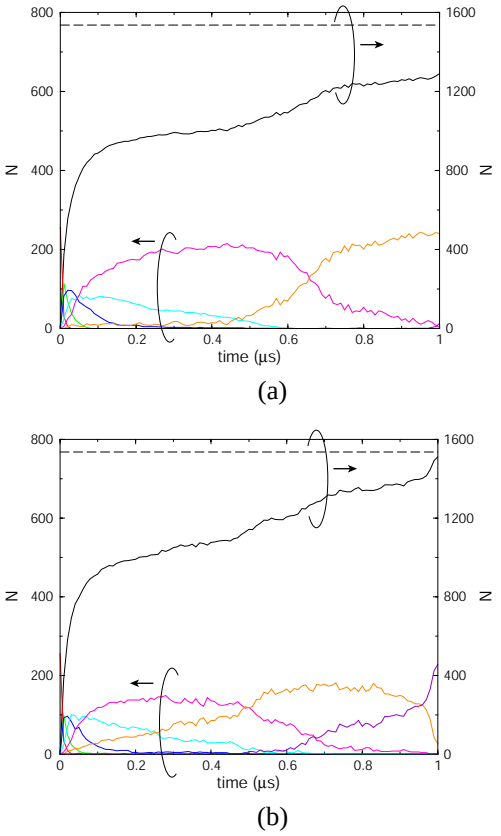

Fig. 6 (a) Time evolution of the number of coordination bonds (black line) and number of zero- to six-coordinated (red, green, blue, cyan, magenta, orange and violet lines, respectively) Ru(II) in the self-assembly process of the [Ru(II)(4,4'-bpy)$_3$] system. (b) Corresponding time evolution with the Ru-N distance enlargement.

with a scaling factor of 1.2 instead of the previous value of 0.78. The corresponding time evolution of the total number of coordination bonds from zero- to six-coordinated Ru(II) are shown in Fig. 6(b). With this enlarged Ru-N$_{bpy}$ distance, six-coordinated Ru(II) became the dominant species and the total number of coordination bonds approached the full-bonding values at t=1.0 μs, as shown in Fig. 6(b). Snapshots in Fig. 7 show the spontaneous growth process of the 3-D MOF. Marked peaks in the radial distribution function (RDF) in Fig. 8 with the enlarged Ru-N distance (red line) show the high structural regularity of the obtained 3-D MOF. Whereas, RDF for the case without the Ru-N distance enlargement (black line) flatten out around the value of one over the distance larger than 3 nm, which corresponds to the structureless uniform distributions of the 4,4'-bpys. We also tried using the Ru-N$_{bpy}$ distance of ca. 0.24 nm and found that it was insufficient to obtain the regular MOF.

Here, we note again the effect of the metal-ligand binding

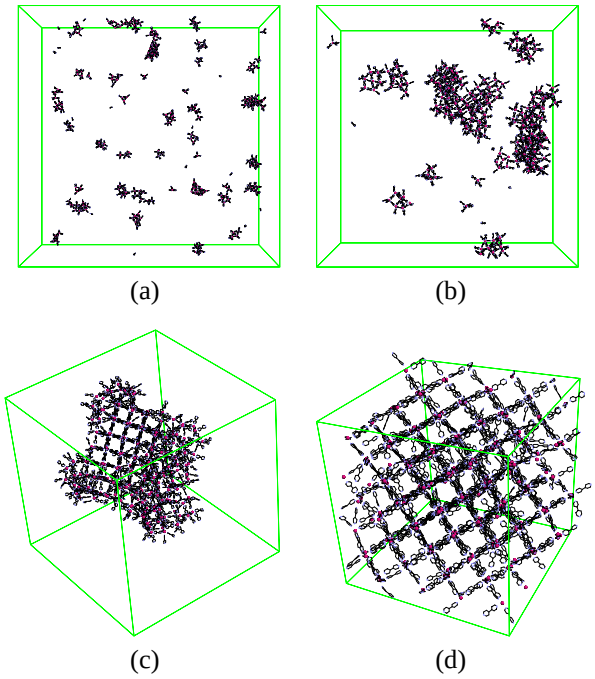

Fig. 7 Snapshot after (a) 0.4 μs, (b) 0.6 μs, (c) 0.8 μs and (d) 1.0 μs of the enlarged Ru-N distance [Ru(II)(4,4'-bpy)$_3$] system simulation (hydrogen atoms are omitted for clarity). Scale (box sizes) are different in these snapshots.

strength upon this 3-D MOF case. The near-field relative dielectric constant ε_r = 1.75 applied in above was the optimum value we found for the regular 3-D MOF self-assembly. With a smaller value, e.g., ε_r = 1.2 (corresponds to the larger metal-ligand binding energy), we obtained the RDF (green line) in Fig. 8 that flatten out again as the case without the Ru-N distance enlargement (black line), even with the enlarged Ru-N distance. This could be the result of too strong metal-ligand binding. In contrast, too weak metal-ligand binding gives no MOF growth, it should be within a window between appropriate values again in this 3-D MOF case.

In summary, we successfully demonstrated the spontaneous growth of 2-D like and 3-D MOFs composed of metal ions and 4,4'-bpys by molecular dynamics simulations. The latter 3-D cubic MOF with octahedral metal centers and 4,4'-bpys has not been experimentally reported to date. Our simulation results show that the metal-N_{bpy} distance is one of the most important factors for realizing such 3-D MOFs and that the distance should be larger than 0.25 nm for the steric requirement around the octahedrally coordinated metals in the 3-D MOFs with 4,4'-bpys. We think this results demonstrated how our simulation model can be used to identify the key design factor to realize a target MOF that has not been previously reported. Our results also show that the metal-ligand binding strength is

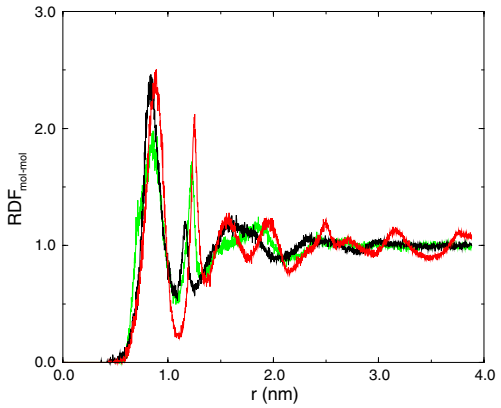

Fig. 8 The 4,4'-bpy center of molecular mass radial distribution functions averaged over the last 100 ps without (black line) and with (red line) the Ru-N distance enlargement and with the Ru-N distance enlargement and also the smaller ε_r = 1.2 (green line).

definitely important and it should be within a window around the optimum values (i.e., not too weak and not too strong) for the regular MOF growth.

Acknowledgment

We would like to thank Prof. Makoto Fujita of the University of Tokyo for valuable discussions.

Notes and References

1 J.-M. Lehn, *Science*, 2002, **295**, 2400–2403
2 M. Tominaga, K. Suzuki, M. Kawano, T. Kusukawa, T. Ozeki, S. Sakamoto, K. Yamaguchi and M. Fujita, *Angew. Chem., Int. Ed.*, 2004, **43**, 5621–5625
3 T. R. Cook, Y.-R. Zheng and P. J. Stang, *Chem. Rev.*, 2012, **113**, 734–777
4 M. Fujita, Y. J. Kwon, S. Washizu and K. Ogura, *J. Am. Chem. Soc.*, 1994, **116**, 1151–1152
5 H. Furukawa, K. E. Cordova, M. OfKeeffe and O. M. Yaghi, *Science*, 2013, **341**, 1230444
6 H.-C. Zhou and S. Kitagawa, *Chem. Soc. Rev.*, 2014, **43**, 5415–5418
7 F. Millange, M. I. Medina, N. Guillou, G. Férey, K. M. Golden and R. I. Walton, *Angew. Chem., Int. Ed.*, 2010, **49**, 763–766
8 J. Cravillon, C. Schröder, R. Nayuk, J. Gummel, K. Huber and M. Wiebcke, *Angew. Chem., Int. Ed.*, 2011, **50**, 8067–8071
9 M. Yoneya, S. Tsuzuki, T. Yamaguchi, S. Sato and M. Fujita, *ACS nano*, 2014, **8**, 1290–1296
10 Y. Pang, *J. Mol. Model.*, 1999, **5**, 196–202
11 M. Yoneya, T. Yamaguchi, S. Sato and M. Fujita, *J. Am. Chem. Soc.*, 2012, **134**, 14401–14407
12 A. Villa, C. Peter and N. F. van der Vegt, *Physical Chemistry Chemical Physics*, 2009, **11**, 2077–2086
13 We think that the box shrinkage at the later low system density stage simply shorten the mean free path of the close encounters between the metals and the ligands. We suppose this free- fright periods does not much affect the coordination-bonding behaviors and then the MOF self-assembly.

14 We first tried cubic box shrinkage with the same shrinkage rates in xyz-directions. However, we found that this shrinkage protocol cause deformation of 2-D like MOF structure under the cubic 3-D periodic boundary condition. Then we applied a tetragonal box shrinkage in which the shrinkage rate in z-direction was three times larger than those in x- and y-directions.

15 S. Roche, C. Haslam, H. Adams, S. L. Heath and J. A. Thomas, *Chem. Commun.*, 1998, 1681–1682

16 J. L. Templeton, *J. Am. Chem. Soc.*, 1979, **101**, 4906–4917

17 A. K. Rappé, C. J. Casewit, K. Colwell, W. Goddard III and W. Skiff, *J. Am. Chem. Soc.*, 1992, **114**, 10024–10035

18 In this case, cubic box shrinkage with the same shrinkage rates in xyz-directions was applied.

19 L. Carlucci, G. Ciani, D. M. Proserpio and A. Sironi, *Angew. Chem., Int. Ed.*, 1995, **34**, 1895–1898

20 D. V. Soldatov and J. A. Ripmeester, *Supramolecular Chemistry*, 1998, **9**, 175–181

21 This is also supported by our corresponding simulation performed using the united-atom 4,4'-bpy model (instead of the all-atom model as above), in which regular 3-D MOFs were spontaneously formed even with the Ru-N_{bpy} distance of ca. 0.21 nm. This could be rationalized by the fact that all the hydrogen atoms of 4,4'-bpys were neglected (as the united-CH_n atoms) in this united-atom model simulation led to the steric problems around Ru(II) being less severe than in the all-atom model simulations.

22 As we stated, the octahedrally coordinated pyridine (py) complex Ru(II)$(py)_6$ has been previously reported even with the Ru-N_{py} distance (ca. 0.21 nm)[16]. We speculate that the py rings in this Ru$(py)_6$ complex can better optimize their configurations (Figure 4 in ref.[16]) to meet the steric requirements than those in the 3-D MOFs under the 3-D network connection constraints.